

# Single Amino Acid Substitutions in the pm2 Muscarinic Receptor Alter Receptor/G Protein Coupling Without Changing Physiological Responses

DYLAN A. BULSECO and MICHAEL I. SCHIMERLIK

Department of Biochemistry and Biophysics (D.A.B., M.I.S.) and the Environmental Health Sciences Center (M.I.S.), Oregon State University, Corvallis, Oregon 97331

Received March 6, 1995; Accepted September 25, 1995

## SUMMARY

The amino terminus of the third cytoplasmic loop of the porcine m2 muscarinic receptor plays an important role in receptor/effector coupling. Although large changes in coupling properties are easily detected, subtle changes are often overlooked. Three mutant receptors were characterized after expression in Chinese hamster ovary cells, and two of these exhibited subtle changes in coupling properties. Substitution of amino acids 219-223 (KDKKE) with those conserved in the m1/m3/m5 receptor subtype family (ELAAL) had little effect on coupling to effector systems, indicating that altering the charge distribution in this region did not affect receptor/G protein interactions. Substitution of alanine with glutamate at amino acid position 212 (A212E) or lysine with alanine in position 214 (K214A)

resulted in receptors with IC<sub>50</sub> values for inhibition of adenylyl cyclase that resembled those of wild-type, although maximal percent inhibition was reduced. All mutants moderately decreased coupling to phosphatidylinositol metabolism, but mutant A212E caused oxotremorine-M to become a weak partial agonist compared with carbachol, suggesting that receptor conformation is agonist dependent even for ligands normally thought of as full agonists. K214A coupled to PI metabolism through both PTX-sensitive and PTX-insensitive G proteins. The results indicated that these mutants superficially possessed effector coupling characteristics similar to those of wild-type, but on more detailed examination G protein/receptor interactions were altered.

mAcChRs mediate intracellular responses through coupling to heterotrimeric G proteins. They are members of a large family of G protein-coupled receptors that possess seven hydrophobic transmembrane regions connected by alternating intracellular and extracellular loops with ligand-binding domains located within the transmembrane regions. Five unique subtypes of mAcChRs (m1-m5) have been cloned and characterized (1-3). The odd-numbered subtypes (m1, m3, and m5) stimulate phospholipid metabolism, whereas the even-numbered subtypes (m2 and m4) preferentially couple to inhibition of adenylyl cyclase (4). The m2 subtype also couples to the inward rectifying K<sup>+</sup> channel in the heart. The m2 muscarinic receptor subtype couples to both inhibition of adenylyl cyclase and stimulation of PI metabolism when expressed in CHO cells (5).

G proteins that mediate the actions of mAcChRs can be distinguished by their sensitivity to ADP ribosylation by PTX. The m2 mAcChR couples to inhibition of adenylyl cy-

clase and stimulation of PI hydrolysis in CHO cells via G proteins with differing PTX sensitivities (5). When m1 and m3 receptor subtypes are expressed in CHO cells, they couple to stimulation of PI hydrolysis either through both PTX-sensitive and -insensitive G proteins or via a G protein with intermediate sensitivity (6). These results indicate that different mAcChR subtypes are capable of evoking similar physiological responses by coupling through different G proteins in the same cell line. Chimeras of i3 or the amino-terminal portion of i3 made with the  $\beta_1$ -adrenergic and m2 receptors indicate that promiscuous receptor G protein coupling occurs with both PTX-sensitive and -insensitive G proteins when the wrong i2 is included (31).

The amino-terminal and carboxyl-terminal regions of i3 have been shown to play important roles in regulation of receptor coupling to G proteins and activation of effector systems for both the muscarinic (7-10) and  $\beta$ -adrenergic (11, 12) receptors. For the mAcChR, the first 15-20 amino-terminal residues of i3 are sufficient to determine selective coupling to G proteins. Wess *et al.* (8) used chimeric m2/m3 receptors stably expressed in A9 L cells to show that the first

This work was supported by National Institutes of Health Grants HL23632 and ES00210.

**ABBREVIATIONS:** mAcChR, muscarinic acetylcholine receptor; pm2, porcine m2 subtype of the muscarinic acetylcholine receptor; i3, third intracellular loop; CHO, Chinese hamster ovary; PI, phosphatidylinositol; PTX, pertussis toxin; Oxo M, oxotremorine-M; *l*-QNB, (-)-quinuclidinylbenzilate; NMS, *N*-methyl scopolamine; IP1, inositol monophosphate; EGTA, ethylene glycol bis( $\beta$ -aminoethyl ether)-*N,N,N',N'*-tetraacetic acid.

17 amino-terminal residues of i3 from the m3 mAChR rendered the m2 subtype PTX insensitive for coupling to PI metabolism, whereas PTX-sensitive inhibition of adenylyl cyclase was retained. This finding suggests that the selectivity determinant for receptor/G protein interaction lies within the first 17 amino-terminal amino acid residues. This domain of i3 is proposed to have  $\alpha$ -helical secondary structure and best correlates with the second messenger preferences exhibited by the odd- and even-numbered receptor subtypes in this region (4, 13). Arden *et al.* (14) reported that substitution of three amino-terminal i3 residues (the 5th, 7th, and 12th) from m1 mAChRs (glutamate, lysine, and glutamate) with residues found in the m2 subtype (alanine, lysine, and lysine) did not alter the characteristics of carbachol-mediated m1 mAChR coupling to PI hydrolysis. In this mutant, the charge distribution was changed to that seen in the m2 mAChR, which couples to inhibition of adenylyl cyclase by a PTX-sensitive G protein. Blüml *et al.* (34, 35) showed that a critical tyrosine at the amino terminal of i3 was necessary for efficient coupling to PI hydrolysis. Carbachol was the only agonist used in these studies, and PTX sensitivity was not assessed.

In the experiments presented below, pm2 mAChRs with mutations in charged residues at the amino terminus of i3 were characterized using carbachol as well as other full and partial agonists (33). The results of these experiments suggest that even single amino acid mutations in this region may subtly affect ligand-binding behavior as well as the manner in which mutant receptors interact with G proteins. Alterations in G protein specificity can be as dramatic as selectively changing the behavior of a full agonist to a partial agonist for PI stimulation but not inhibition of cAMP formation or as subtle as altering the sensitivity of a response to uncoupling by PTX, suggesting interaction with additional G protein(s). Taken together, these results emphasize the difficulty in assigning precise structural domains in i3 of the pm2 mAChR without thorough receptor characterization.

## Experimental Procedures

**Materials.**  $l$ -[ $^3$ H]QNB (43 Ci/mmol), [ $^3$ H]NMS (79 Ci/mmol), and *myo*-[ $^3$ H]inositol (17.8 Ci/mmol) were purchased from DuPont-New England Nuclear. Carbachol and atropine were purchased from Aldrich Chemical Company, and  $l$ -QNB, NMS, Oxo M, acetylcholine, and pilocarpine were obtained from Research Biochemicals International. Glass-fiber filters were from Schleicher & Schuell (No. 32) or Whatman (GF/B). Restriction enzymes and T4 DNA polymerase were from Promega, GIBCO-Bethesda Research Laboratories, or New England Biolabs. The mammalian expression vector (pSVE) and the clone for the wild-type pm2 mAChR were gifts from Genentech, Inc. The dhfr<sup>-</sup> CHO cells were obtained from America Type Culture Collection. PTX was from List Biological Laboratories, and 4-(3-butoxy-4-methoxybenzyl)-2-imidazolidinone was from Bio Mol Research Labs.

**Site-directed mutagenesis and expression.** Site-directed mutagenesis was carried out as described by the mutagenesis procedure of Bio-Rad. After cloning the gene for the pm2 mAChR into the *Hind*III/*Eco*RI sites of the polylinker region of m13mp18, uracil containing single-stranded DNA was annealed to mutagenic primers. The primers for A212E (5'-CCTGCTCTTACTTTCCCGG-GATATGTGC-3') and K214A (5'-GTCCTTCTTAATTCTAGAG-GCACTGGCTCGGGA-3') were designed to introduce a single amino acid change as well as new restriction enzyme sites to facilitate

screening for mutants. The mutagenic oligonucleotide primer 5'-CTCCTTAATCCTGCTCTCACTCTCCCGGATATGTGCCA-3' was designed to replace five amino acids in position 219–223 (KD-KKE(219–223)ELAAL). After mutant clones were identified, the mutations were confirmed by dideoxy DNA sequencing (15).

The *Hind*III/*Eco*RI fragment containing the pm2 mAChR coding region was isolated from m13mp18 Rf DNA by agarose gel electrophoresis and subcloned into the multiple cloning region of the expression vector pSVE (3). Mutant pm2 mAChR-pSVE constructs were transfected into dhfr<sup>-</sup> CHO cells by calcium phosphate precipitation. Cells expressing recombinant receptor were grown in selective media (modified Dulbecco's modified Eagle's medium low in glycine and thymine) with 10% dialyzed calf serum, 100 mg/ml insulin, and methotrexate. Increasing concentrations of methotrexate resulted in amplification of receptor expression.

Receptor expression was assessed in whole cells on tissue culture dishes by the addition of 10 nM  $l$ -[ $^3$ H]QNB or [ $^3$ H]NMS in the presence or absence of 100 mM atropine or 1 mM unlabeled  $l$ -QNB. Cells were incubated for 1.5 hr at 37° and then washed twice with ice-cold phosphate-buffered saline, pH 7.4. Cells were solubilized with 1 ml of 1% Triton X-100 in phosphate-buffered saline and then counted for tritium. Once receptors were expressed, membranes were prepared, and binding of ligands was assayed as described below.

**Membrane preparation and ligand binding.** Suspension cultures were grown in modified Dulbecco's modified Eagle's medium low in glycine and thymine at 37° in spinner culture flasks. Cells were harvested, and the pellet was resuspended in two volumes of homogenization buffer (250 mM sucrose, 50 mM EDTA, 25 mM imidazole buffer, pH 7.4) containing benzamidine, soybean trypsin inhibitor, and pepstatin A at final concentrations of 1 mg/ml. The cell suspension was homogenized with a polytron homogenizer, PTA 10S probe, for 2 × 20 sec at 4° under argon, and cell membranes were prepared by sucrose gradient centrifugation as previously described (16). In some cases, 5 mM Na butyrate was added 24 hr before harvesting cells to further enhance receptor expression. Untreated and butyrate-treated cultures resulted in membrane preparations with specific activities of 20–300 pmol NMS sites/mg protein. All ligand-binding experiments were conducted in buffer containing 10 mM HEPES, 5 mM MgCl<sub>2</sub>, 1 mM EDTA, and 1 mM EGTA, pH 7.4, at 25° by displacement of either  $l$ -[ $^3$ H]QNB or [ $^3$ H]NMS. Samples were filtered through glass-fiber filters and washed three times with 4 ml of ice-cold 50 mM Na phosphate buffer, pH 7.4. When [ $^3$ H]NMS was used, the glass-fiber filters were treated with 0.1% (w/v) polyethyleneimine before use. Nonspecific binding was determined in the presence of 10<sup>-4</sup> M  $l$ -hyoscyamine and was <10% of the total radiolabel bound.

**Assays for effector coupling.** Stably transfected CHO cells expressing wild-type or mutant pm2 mAChRs were assayed in 24-well dishes for agonist-stimulated PI metabolism. Cells were plated at an initial density of 2.0 × 10<sup>6</sup> cells per well in Dulbecco's modified Eagle's medium with F-12 Nutrient Mixture (GIBCO-Bethesda Research Laboratories) and 10% calf serum (Sigma) and, after addition of 0.5 ml of media containing 1  $\mu$ Ci/ml *myo*-[ $^3$ H]inositol per well, incubated at 37° for 24 hr. IP1 accumulation was measured as described by Lee *et al.* (17) 30 min after the addition of ligands. To maximize fold-stimulation of PI metabolism when constructing PTX dose-response curves, IP1 accumulation was measured 50 min after carbachol addition.

Assays for inhibition of forskolin-stimulated cAMP levels were conducted on CHO cells expressing wild-type or mutant receptors by a modification of the Salomon method (18). Cells were plated on 35-mm tissue culture dishes and grown to a final density of 1.0 × 10<sup>6</sup> cells/plate. Before the assay for cAMP, cells were incubated with [ $^3$ H]adenine (1  $\mu$ Ci/ml) for 2 hr in the presence of 0.5 mM 4-(3-butoxy-4-methoxybenzyl)-2-imidazolidinone at 37° in Dulbecco's modified Eagle's medium plus F12 Nutrient Mixture. Total tritium labeled cAMP was separated with successive columns of AG50W-X4 resin (Bio-Rad) and Alumina (Sigma). The cAMP was eluted from the

alumina columns directly into scintillation vials with 4 ml of 0.1 M imidazole buffer, pH 7.4, and samples were counted in a liquid scintillation counter. In specific experiments, PTX was added 6–12 hr before the assay to give the appropriate final concentration.

Initial experiments indicated that in CHO cells expressing wild-type pm2 mAChR over the range of  $10^5$  to  $2 \times 10^6$  receptors per cell, the  $IC_{50}$ , but not the maximal inhibition, for cAMP formation and the maximal fold stimulation, but not the  $EC_{50}$ , for PI stimulation were dependent on the number of receptors per cell (33). Thus, it was necessary to compare the  $IC_{50}$  for adenylyl cyclase inhibition and the maximal fold stimulation of PI metabolism of mutants with wild-type cell lines containing an approximately identical number of receptors per cell. After many attempts, it was not possible to isolate an appropriate distribution of cell lines, nor was it possible to reduce wild-type receptor number sufficiently with the alkylating agent benzylcholine mustard, which was able to maximally remove ~90% of the surface sites from wild-type pm2 mAChR cell lines expressing  $1-2 \times 10^6$  sites/cell. An alternative approach in which receptor number was reduced by addition of various amounts of the slowly dissociating antagonist *l*-QNB was used. After 1 hr, the plates were rinsed twice with media to remove any free *l*-QNB. The physiological assays were then initiated with the appropriate agonists, and the average numbers of surface receptors per cell was determined by the addition of [ $^3$ H]NMS in the presence or absence of  $10^{-4}$  M *l*-hyoscyamine. Plots of  $IC_{50}$  (for inhibition of cAMP formation) and fold-maximal response (for PI stimulation) versus pm2 receptors/cell were made, and the appropriate wild-type parameter was determined from the standard curves and used for comparison with the values for mutants expressing receptors at the same receptor number per cell. Parameters for mutant receptors were compared with wild-type pm2 mAChR expressed at the appropriate receptor density (Tables 1 and 2).

**Data analysis.** Functional assays and agonist ligand-binding data were analyzed with the use of nonlinear least-squares curve fitting in Origin (MicroCal Software). Data from effector coupling

TABLE 1  
Mutant pm2 mAChR coupling to stimulation of inositol phospholipid metabolism

Agonist	log $EC_{50}$	Maximal fold stimulation	n
	M		
Carbachol			
Wild-type	$5.8 \pm 0.2$	(1.60, 1.63, 1.72) <sup>b</sup>	•
A212E	$5.6 \pm 0.3$	$1.6 \pm 0.1$	7
K214A	$5.5 \pm 0.3$	$1.9 \pm 0.2$	5
KDKKE(219–223)ELAAL	$5.3 \pm 0.3^d$	$2.0 \pm 0.3$	7
Acetylcholine			
Wild-type	$6.5 \pm 0.4$	(1.65, 1.70, 1.82) <sup>b</sup>	•
A212E	$6.1 \pm 0.1$	$1.43 \pm 0.04^d$	6
K214A	$5.6 \pm 0.5^d$	$1.7 \pm 0.5$	11
KDKKE(219–223)ELAAL	$5.4 \pm 0.2^d$	$1.8 \pm 0.2$	4
Oxo M			
Wild-type	$7.1 \pm 0.9$	(1.50, 1.52, 1.62) <sup>b</sup>	•
A212E	<sup>c</sup>	$1.3 \pm 0.1^d$	6
K214A	$6.5 \pm 0.9$	$1.8 \pm 0.1$	7
KDKKE(219–223)ELAAL	$6.3 \pm 0.3$	$1.8 \pm 0.2$	5
Pilocarpine			
Wild-type	$4.6 \pm 0.7$	(1.25, 1.30, 1.58) <sup>b</sup>	•
A212E	<sup>c</sup>	$1.2 \pm 0.1$	2
K214A	<sup>c</sup>	$1.10 \pm 0.01^d$	2
KDKKE(219–223)ELAAL	$4.9 \pm 0.1$	$1.4 \pm 0.1$	2

• Values represent the mean  $\pm$  standard deviation of 3 to 12 experiments.

<sup>b</sup> Wild-type percent maximal stimulation at  $3 \times 10^5$ ,  $3.8 \times 10^5$ , and  $1.0 \times 10^6$  pm2 mAChR/cell.

<sup>c</sup>  $EC_{50}$  is not well determined due to small observed response to agonist treatment.

<sup>d</sup> Significantly different from pm2 wild-type mAChR expressed at comparable receptor densities ( $p < 0.01$ , Student's *t* test).

TABLE 2

Mutant pm2 mAChR coupling to inhibition of cAMP formation

Agonist	log $IC_{50}$	Maximal inhibition	n
	M	%	
Carbachol			
Wild-type	(6.5, 6.6, 7.0) <sup>b</sup>	$74 \pm 7$	•
A212E	$6.1 \pm 0.3$	$48 \pm 9^c$	6
K214A	$6.8 \pm 0.9$	$47 \pm 4^c$	6
KDKKE(219–223)ELAAL	$7.2 \pm 0.5$	$48 \pm 4^c$	9
Acetylcholine			
Wild-type	(7.4, 7.5, 8.0) <sup>b</sup>	$74 \pm 7$	•
A212E	$6.8 \pm 0.3^c$	$36 \pm 7^c$	3
K214A	$7.0 \pm 0.1^c$	$42 \pm 7^c$	4
KDKKE(219–223)ELAAL	$7.6 \pm 0.4$	$45 \pm 7^c$	3
Oxo M			
Wild-type	(6.9, 7.0, 7.4) <sup>b</sup>	$73 \pm 6$	•
A212E	$6.4 \pm 0.4$	$39 \pm 4^c$	3
K214A	$6.7 \pm 0.4$	$42 \pm 3^c$	3
KDKKE(219–223)ELAAL	$7.96 \pm 0.04$	$48 \pm 2^c$	2

• Values represent the mean  $\pm$  standard deviation of three or four experiments.

<sup>b</sup> Wild-type  $EC_{50}$  values at  $3.0 \times 10^5$ ,  $3.8 \times 10^5$ , and  $1.0 \times 10^6$  pm2 mAChRs/cell.

<sup>c</sup> Significantly different from pm2 wild-type mAChR expressed at comparable receptor densities ( $p \leq 0.01$ , Student's *t* test).

assays were either fit to the logistic eq. 1 for PI assays or eq. 2 for cAMP assays.

$$Y = A + \frac{(B - A)}{1 + (C/[x])^D} \quad (1)$$

$$Y = A + \frac{(B - A)}{1 + (C/[x])^D} + \frac{(E - A)}{1 + ([x]/F)^G} \quad (2)$$

For each of these equations,  $[x]$  is the ligand concentration;  $A$  and  $B$  (or  $E$ ) are the minimum and maximum plateaus of the curve, respectively;  $C$  is the  $EC_{50}$  for PI or adenylyl cyclase stimulation;  $F$  is the  $IC_{50}$  for adenylyl cyclase inhibition; and  $D$  (or  $G$ ) is the Hill coefficient or slope factor. The logistic equation is customarily used to evaluate dose-response curves (36). Competition displacement curves were fit according to a mass action model for receptor/ligand interactions at three independent classes of sites (eq. 3) as described in Tota *et al.* (19).

$$Y = \left( \frac{[L]}{K} \right) \left[ \frac{(F_1)}{1 + [L]/K + [I]/K_1} + \frac{(F_2)}{1 + [L]/K + [I]/K_2} + \frac{(1 - F_1 - F_2)}{1 + [L]/K + [I]/K_3} \right] \quad (3)$$

In eq. 3,  $Y$  is the fractional saturation of the receptor, and  $[L]$  is the free concentration of antagonist used in the experiment with dissociation constant  $K$ .  $[I]$  is the total concentration (assumed to equal the free concentration since significant displacement does not occur until  $[I \text{ total}] \gg [\text{total receptor}]$ ) of the competing agonist with dissociation constants  $K_1$ ,  $K_2$ , and  $K_3$ .  $F_1$ ,  $F_2$ , and  $F_3$  are the corresponding fractions of total binding sites where  $F_3 = 1 - F_1 - F_2$ . Antagonist binding was analyzed using Scatchard plots (20). Student's *t* test ( $p \leq 0.01$ ) was used to assess statistical significance.

## Results

**Expression of pm2 receptors in CHO cells.** The pm2 mAChR constructs in pSVE were stably transfected into dhfr<sup>-</sup> CHO cells and amplified by growing in the presence of increasing concentrations of methotrexate. The wild-type pm2 cell line expressed  $1.2 \times 10^6$  total receptors per cell, whereas A212E, K214A, and KDKKE(219–223)ELAAL expressed  $3.0 \times 10^5$ ,  $3.8 \times 10^5$ , and  $1.0 \times 10^6$  receptors/cell, respectively. Comparison of specific [ $^3$ H]NMS versus [ $^3$ H]QNB binding indicated that wild-type and KD-



KKE(219–223)ELAAL expressed 100% of their receptors on the cell surface, and A212E and K214A expressed ~70–80%.

**Ligand-binding characteristics.** The ligand-binding properties of pm2 mutants and wild-type receptor are summarized in Table 3. The affinity of  $l$ -[ $^3$ H]QNB was within a factor of 2 for the mutants compared with wild-type, whereas [ $^3$ H]NMS binding was weaker to the mutants by 3–5-fold. Thus, the antagonist-binding properties of the mutants for these two ligands were affected in the mutant pm2 receptors but not very strongly.

Agonist-binding data for wild-type pm2 mAChR for carbachol, acetylcholine, and Oxo M were consistent with fits to three independent classes of sites ( $K_1$ ,  $K_2$ , and  $K_3$ ), whereas pilocarpine data were best fit by assuming two classes of sites (i.e.,  $K_2 = K_3$ ). Agonist-binding properties were affected in a selective manner by specific mutations. The mutation A212E appears to reduce the affinity of the pm2 mAChR for acetylcholine but not carbachol and slightly increased the affinity for Oxo M. The mutation K214A increased the affinity for Oxo M by 5–27-fold. The mutation KDKKE(219–223)ELAAL also increased the affinity for Oxo M at the low and intermediate affinity sites and for carbachol at the high affinity site by factors of 8–10-fold. The binding properties of the partial agonist pilocarpine were essentially unaffected for the three mutants.

**Stimulation of PI metabolism.** Data comparing the coupling of wild-type and mutant pm2 mAChRs to stimulation of PI are summarized in Fig. 1a and Table 1. Carbachol, acetylcholine, and Oxo M stimulated accumulation of IP1 up to 2-fold over basal levels in cells expressing wild-type pm2 mAChRs.  $EC_{50}$  values for these agonists were 1.7, 0.3, and

0.1  $\mu$ M, respectively. The maximal fold stimulation values reported for wild-type pm2 mAChRs are those estimated from the standard curve at  $3.0 \times 10^5$ ,  $3.8 \times 10^5$ , and  $1.0 \times 10^6$  receptors/cell, respectively, and mutant pm2 mAChRs at their respective receptor densities.

Compared with wild-type, the mutant pm2 mAChRs stimulated PI hydrolysis with  $EC_{50}$  values that are selectively altered, depending on the ligand and mutant. Wild-type receptor, A212E, K214A, and KDKKE(219–223)ELAAL display  $EC_{50}$  values of 1.7, 2.5, 3.5, and 5.7  $\mu$ M, respectively, when carbachol is the agonist, with maximal percent stimulation of 60–72%, 63%, 85%, and 98%. These findings indicate that these mutants have little or no effect on carbachol-mediated coupling to PI metabolism.

Acetylcholine and Oxo M appear to have different effects on the coupling of mutants to stimulation of PI metabolism than carbachol. Although K214A coupled to PI metabolism with an  $EC_{50}$  value of ~10-fold higher than wild-type for acetylcholine, the  $EC_{50}$  value for Oxo M did not significantly differ. This was also observed for KDKKE(219–223)ELAAL but not A212E.

Although A212E shows high affinity binding to both carbachol and Oxo M (Table 3), Oxo M does not stimulate PI hydrolysis in the same manner as other ligands. Carbachol gave maximal fold stimulation of IP1 formation at levels similar to wild-type with an  $EC_{50}$  of 2.5  $\mu$ M. On the other hand, both acetylcholine and Oxo M behaved like partial agonists for PI stimulation (Figs. 1 and 2), although maximal inhibition of cAMP formation was similar to carbachol (Table 2, Figs. 1b and 3). Maximum fold stimulation significantly differed from wild-type for both of these agonists (Table 1)

TABLE 3  
Ligand binding properties of mutant pm2 mAChRs<sup>a</sup>

Antagonist	l-QNB		NMS	
	p <i>K</i> <sub>d</sub>	<i>n</i>	p <i>K</i> <sub>d</sub>	<i>n</i>
Wild-type	<sup>M</sup> 10.68 ± 0.04	3	<sup>M</sup> 8.9 ± 0.1	3
A212E	10.5 ± 0.1	6	8.1 ± 0.1 <sup>b</sup>	4
K214A	10.6 ± 0.1	3	8.4 ± 0.1 <sup>b</sup>	3
KDKKE(219–223)ELAAL	10.33 ± 0.04 <sup>b</sup>	6	8.3 ± 0.1	2

Agonist	p <i>K</i> <sub>1</sub>	p <i>K</i> <sub>2</sub>	p <i>K</i> <sub>3</sub>	F <sub>1</sub>	F <sub>2</sub>	<i>n</i>
	<sup>M</sup>					
Carbachol						
Wild-type	8.1 ± 0.2	5.6 ± 0.3	4.3 ± 0.1	0.20 ± 0.05	0.52 ± 0.10	4
A212E	8.3 ± 0.1	5.3 ± 0.1	4.4 ± 0.2	0.21 ± 0.02	0.31 ± 0.14	3
K214A	8.42 ± 0.02 <sup>b</sup>	6.0 ± 0.1	5.1 ± 0.1 <sup>b</sup>	0.31 ± 0.02	0.48 ± 0.03	4
KDKKE(219–223)ELAAL	9.0 ± 0.2 <sup>b</sup>	5.7 ± 0.2	4.5 ± 1	0.25 ± 0.04	0.50 ± 0.07	4
Acetylcholine						
Wild-type	9.3 ± 0.1	6.6 ± 0.2	5.2 ± 0.1	0.36 ± 0.02	0.52 ± 0.03	2
A212E	8.0 ± 0.2 <sup>b</sup>	5.3 ± 0.1 <sup>b</sup>	4.4 ± 0.2 <sup>b</sup>	0.25 ± 0.09	0.54 ± 0.25	4
K214A	8.9 ± 0.2	6.7 ± 0.1	5.9 ± 0.2	0.37 ± 0.08	0.32 ± 0.08	2
KDKKE(219–223)ELAAL	9.5 ± 1.1	7.2 ± 0.3	5.4 ± 0.3	0.12 ± 0.06	0.39 ± 0.07	5
Oxo M						
Wild-type	8.3 ± 0.1	6.1 ± 0.1	4.7 ± 0.2	0.17 ± 0.05	0.13 ± 0.08	3
A212E	8.3 ± 0.3	6.7 ± 0.6	5.2 ± 0.1 <sup>b</sup>	0.23 ± 0.01	0.50 ± 0.02	4
K214A	9.0 ± 0.1 <sup>b</sup>	6.76 ± 0.03 <sup>b</sup>	6.2 ± 0.2 <sup>b</sup>	0.15 ± 0.01	0.57 ± 0.08	4
KDKKE(219–223)ELAAL	8.2 ± 0.1	7.7 ± 0.1 <sup>b</sup>	5.7 ± 0.1 <sup>b</sup>	0.25 ± 0.02	0.4 ± 0.03	2
Pilocarpine						
Wild-type	6.6 ± 0.2	4.9 ± 0.3		0.29 ± 0.11	0.71 ± 0.11	3
A212E	6.8 ± 0.1	5.6 ± 0.1		0.53 ± 0.12	0.47 ± 0.10	2
K214A	6.6 ± 0.2	5.2 ± 0.2		0.52 ± 0.05	0.48 ± 0.09	2
KDKKE(219–223)ELAAL	6.5 ± 0.2	5.6 ± 0.2		0.20 ± 0.04	0.80 ± 0.10	2

<sup>a</sup> Values represent the mean  $\pm$  standard deviation of two to four experiments.

<sup>b</sup> Significantly different from pm2 wild-type mAChR ( $p < 0.01$ , Student's  $t$  test).

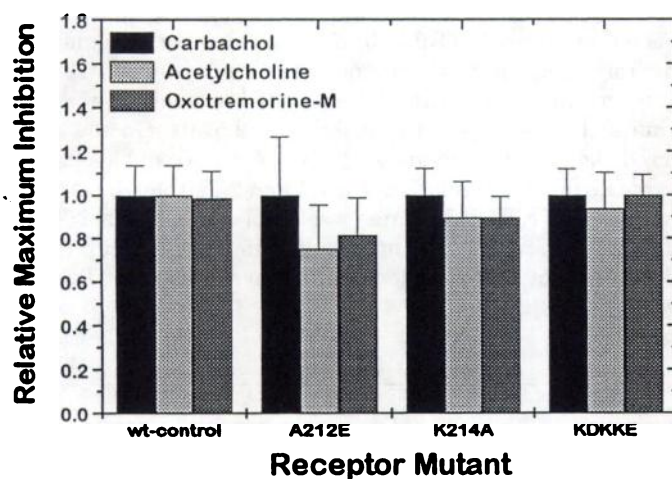
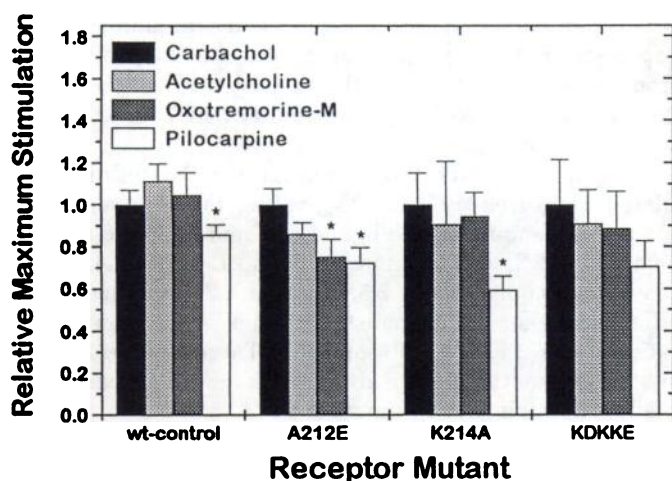


**Fig. 1.** Normalized agonist-mediated maximum stimulation of PI hydrolysis and maximum inhibition of adenylyl cyclase. Experiments were conducted as described in Experimental Procedures. Data are presented as the ratio of agonist-mediated maximal response relative to carbachol-mediated response for each receptor mutant, with associated propagated errors (39). Expression levels are  $1.2 \times 10^6$  receptors/cell for pm2 mAcChR and  $3.0 \times 10^5$ ,  $3.8 \times 10^5$ , and  $1.0 \times 10^6$  receptors/cell for A212E, K214A, and KDKKE(219–223)ELAAL, respectively. A, Normalized maximum PI response. The data shown are from 2–10 experiments done in duplicate ( $\pm$  standard deviation). Pilocarpine-stimulated PI hydrolysis between 59% and 86% of carbachol-stimulated levels, whereas Oxo M and acetylcholine stimulated 89–100%. The one exception was Oxo M for A212E, which maximally stimulated PI hydrolysis at 75% of carbachol-stimulated levels. B, Normalized maximum adenylyl cyclase inhibition. The data shown are from two to nine experiments done in duplicate ( $\pm$  standard deviation). All agonists inhibited cAMP formation between 75% to 100% of carbachol inhibition. \*, Agonists exhibiting statistically significant differences ( $p \leq 0.01$ , Student's *t* test) when compared with carbachol. In addition, Oxo M did not significantly differ from pilocarpine ( $p = 0.37$ ) for the mutant A212E.

with an increase in  $EC_{50}$  for acetylcholine. The response for Oxo M was consistently too low to accurately determine this parameter.

To compare the relative efficacy of agonists for each mutant receptor, maximal stimulation of IP1 accumulation and

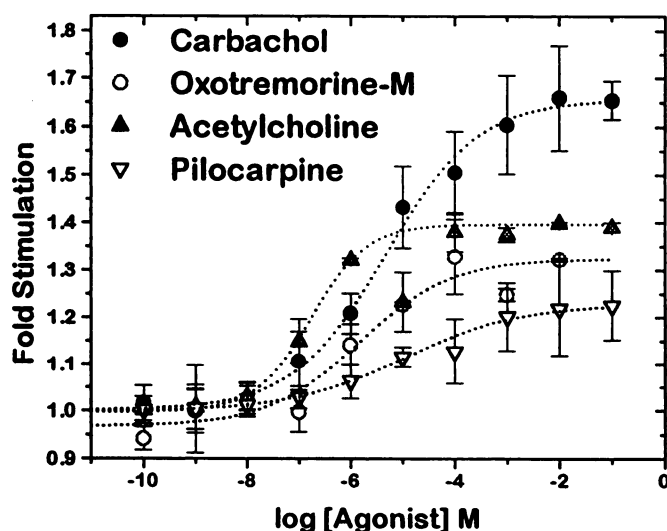
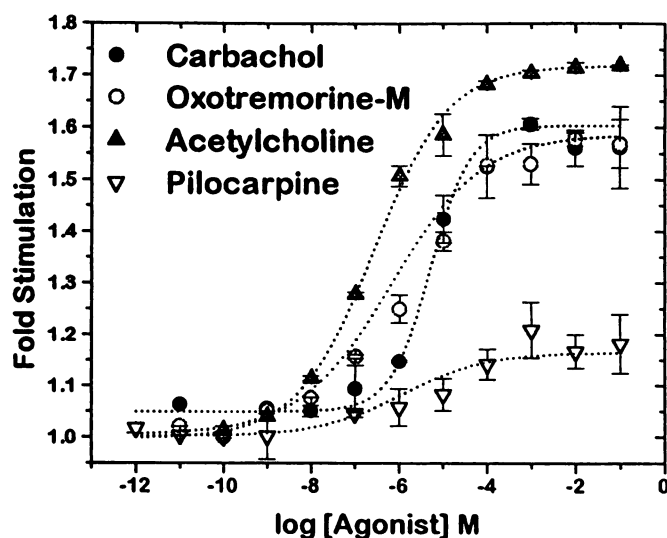


**Fig. 2.** Agonist stimulation of PI hydrolysis by wild-type pm2 AChR and A212E. Experiments were conducted as described in Experimental Procedures. Data are presented as fold stimulation of PI hydrolysis over basal levels of released inositol monophosphates. The data shown are representative of three to six experiments with each agonist concentration done in duplicate. Curves were derived from a least-squares fit to eq. 1 and average values for  $EC_{50}$  and maximal fold stimulation are summarized in Table 1. *Top*, wild-type pm2 mAcChR, expressing  $1.2 \times 10^6$  receptors/cell. The fitted parameters were  $EC_{50} = 4.9 \pm 1.4 \mu M$ , 1.6-fold;  $EC_{50} = 0.59 \pm 0.09 \mu M$ , 1.6-fold;  $EC_{50} = 0.24 \pm 0.02 \mu M$ , 1.7-fold; and  $EC_{50} = 1.4 \pm 1.9 \mu M$ , 1.2-fold for carbachol, Oxo M, acetylcholine, and pilocarpine, respectively. Slope factors used were 1.0 for carbachol and 0.5 for Oxo M, acetylcholine, and pilocarpine. *Bottom*, A212E m2 mAcChR mutant,  $3 \times 10^5$  receptors/cell with fitted parameters of  $EC_{50} = 7.1 \pm 3.9 \mu M$ , 1.7-fold;  $EC_{50} = 2.0 \pm 0.4 \mu M$ , 1.3-fold;  $EC_{50} = 0.17 \pm 0.07 \mu M$ , 1.4-fold; and  $EC_{50} = 24.0 \pm 16.1 \mu M$ , 1.2-fold for carbachol, Oxo M, acetylcholine, and pilocarpine, respectively. Slope factors were 1.0 for carbachol and acetylcholine and 0.5 for Oxo M and pilocarpine.

maximal inhibition of adenylyl cyclase were normalized to the value obtained for carbachol (Fig. 1) for that mutant. Pilocarpine stimulated PI hydrolysis between 59% and 93%

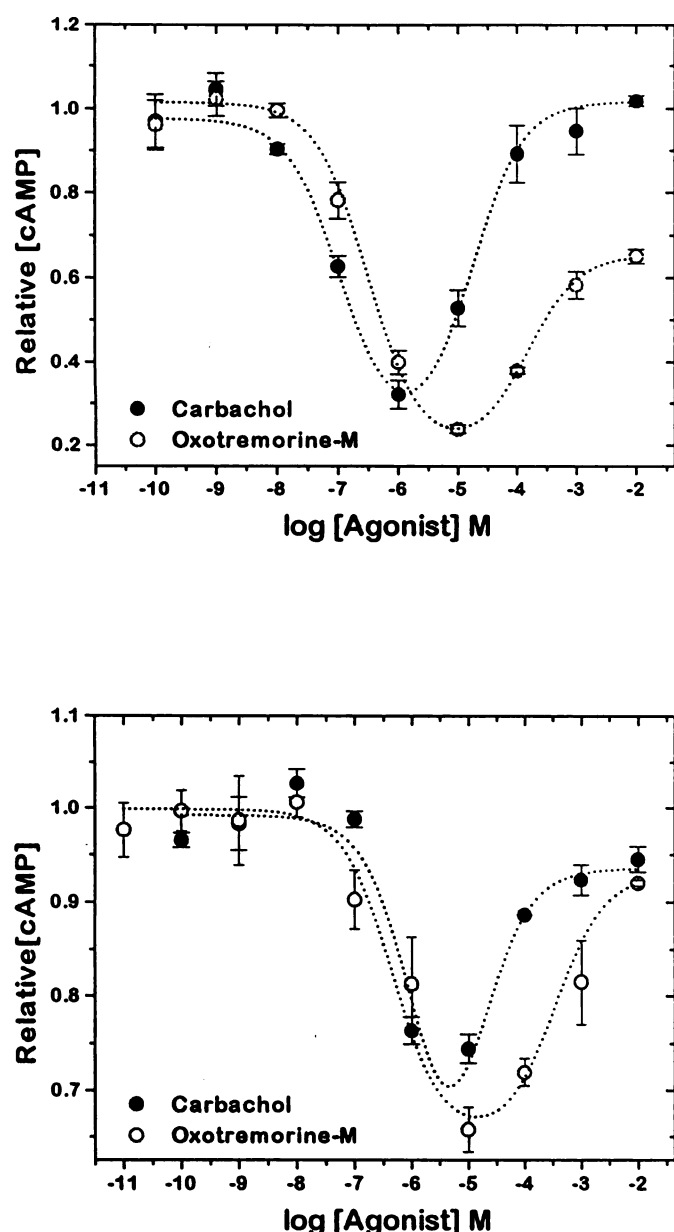


**Fig. 3.** Inhibition of cAMP formation by wild-type pm2 mAChR and A212E. Experiments were conducted as described in Experimental Procedures. Data are presented as levels of cAMP generated relative to forskolin-stimulated levels. The data shown are representative of three or four experiments with duplicate data points. Curves were derived from a least-squares fit to eq. 2, and average values for  $IC_{50}$  and percent maximal inhibition are summarized in Table 2. *Top*, wild-type pm2 mAChR,  $1.2 \times 10^6$  receptors/cell. The fitted parameters were  $IC_{50} = 0.11 \pm 0.03 \mu M$ , 75% inhibition for carbachol; and  $IC_{50} = 0.3 \pm 0.1 \mu M$ , 80% inhibition for Oxo M. *Bottom*, A212E pm2 mAChR mutant,  $3 \times 10^5$  receptors/cell, with fitted parameters of  $IC_{50} = 0.7 \pm 0.3 \mu M$ , 40% inhibition for carbachol; and  $IC_{50} = 0.3 \pm 0.1 \mu M$ , 35% inhibition for Oxo M. Slope factor was 1.0 for both agonists in wild-type and A212E.

of carbachol stimulated levels, whereas Oxo M and acetylcholine stimulated 89–100% compared with carbachol for all receptors characterized. The one exception was Oxo M for A212E, which maximally stimulated PI hydrolysis at 75% of carbachol-stimulated levels. Although the observed maximal stimulation by acetylcholine significantly differed from wild-

type for A212E (Table 1, Fig. 2), it did not appear to differ significantly from carbachol-stimulated levels for this mutant (Fig. 1a). In addition, Oxo M-stimulated levels significantly differ ( $p \leq 0.05$ , Student's *t* test) from pilocarpine levels for all receptors characterized except A212E ( $p > 0.05$ ).

**Inhibition of cAMP formation.** Data describing the coupling of wild-type and mutant pm2 mAChRs to the inhibition of cAMP formation in CHO cells are summarized in Fig. 1b and Table 2. Reduced maximal percent inhibition was observed for all agonists for each of the mutant receptors characterized, although  $IC_{50}$  values for carbachol were similar to wild-type pm2 mAChRs expressed at the same level (Table 2). It is unclear if this finding reflects any specific changes in receptor/G protein interaction or if a general reduction in coupling efficiency is observed due to the slight modifications of i3. This explanation is consistent with the observation that most chimeric receptors couple to effector systems with lower efficiency than the wild-type receptor (10). Unlike the results for stimulation of PI metabolism, maximal inhibition of adenylyl cyclase relative to carbachol was the same for all mutants (Fig. 1b).

Increased  $IC_{50}$  values were observed for acetylcholine for both A212E and K214A, although no significant deviation from wild-type was observed for Oxo M or carbachol. KD-KKE(219–223)ELAAL did not exhibit an agonist-dependent increase in  $IC_{50}$ .

The data in Fig. 3 showed that muscarinic agonists caused both inhibitory and stimulatory effects on cAMP levels. At high concentrations, all agonists appeared to mediate stimulation of adenylyl cyclase. The  $EC_{50}$  of stimulation for the pm2 mAChR was variable and highly dependent on receptor number, with values ranging from 10 to 1000  $\mu M$ .

**PTX sensitivity.** Selectivity of G protein coupling appeared to be affected by removal of a positive charge at the seventh amino-terminal residue of i3 in the mutant K214A. Inhibition of cAMP formation was mediated by a PTX-sensitive G protein for K214A (data not shown), whereas coupling to PI metabolism occurred through G proteins with different PTX sensitivity than wild-type pm2 mAChRs (Figs. 4 and 5). Wild-type receptor, KD-KKE(219–223)ELAAL (Fig. 4), and A212E (data not shown) coupled to PI metabolism by a G protein that was PTX sensitive since treatment with 100 ng/ml PTX for 12 hr resulted in complete uncoupling. For K214A, treatment with 100 ng/ml PTX failed to significantly reduce the measured accumulation of IP1 (Fig. 4), although the  $EC_{50}$  for carbachol was shifted to the left by ~20-fold.

The PTX concentration dependence on maximal fold IP1 accumulation was assessed for K214A and wild-type receptor (Fig. 5). Although PTX treatment reduced the fold accumulation of IP1 for K214A, there was a 100-fold rightward shift in PTX sensitivity compared with wild-type. In addition, treatment with 1000 ng/ml PTX failed to completely abolish the response to carbachol. To maximize the carbachol-stimulated increase in PI hydrolysis, these experiments were allowed to proceed for 50 min instead of 30. Although this may explain the greater fold accumulation of IP1 for both wild-type pm2 receptor and K214A, it does not account for the apparent difference in PTX sensitivity.



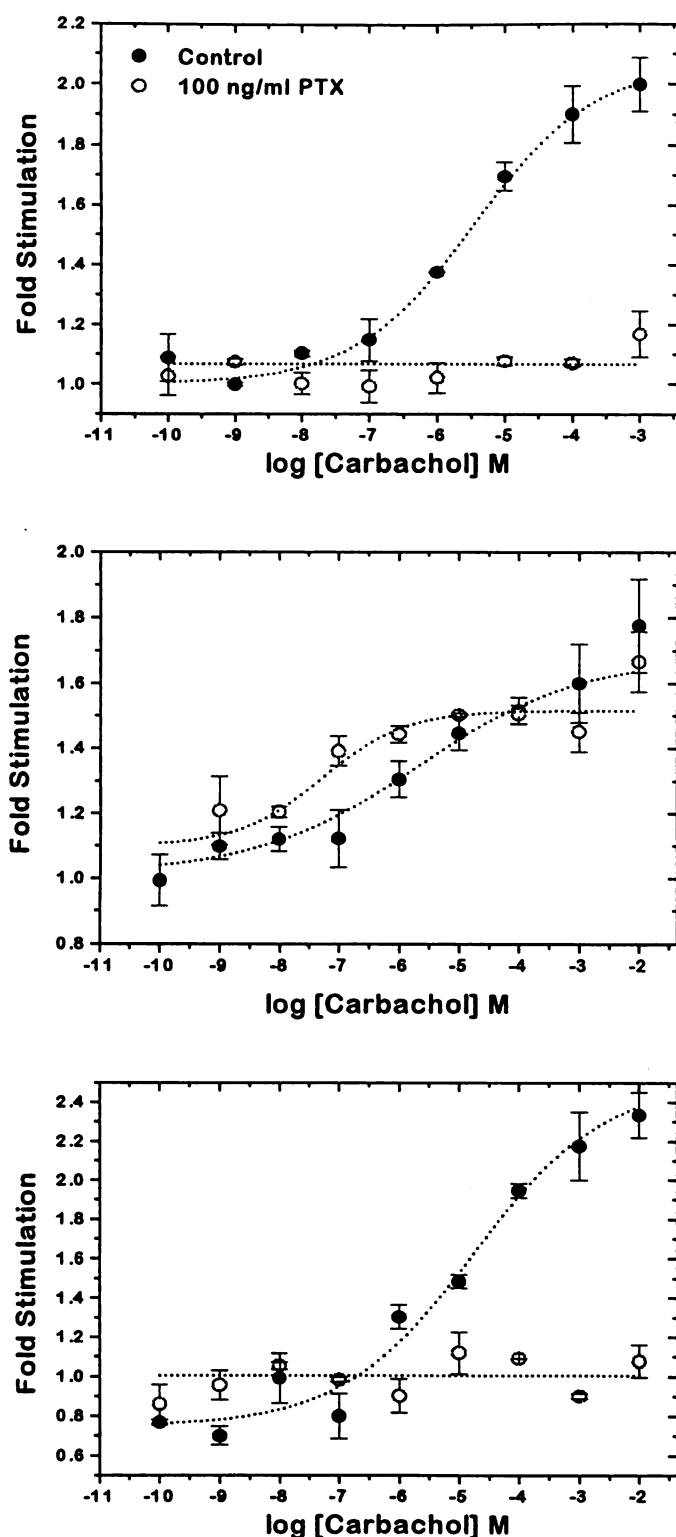


**Fig. 4.** Effect of PTX on PI hydrolysis by wild-type and mutant m2 mAChRs. Cells expressing wild-type or mutant pm2 mAChRs were treated with 100 ng/ml PTX for 12 hr in the presence of 1  $\mu$ Ci/ml myo-[ $^3$ H]inositol before the assay. Data are presented as fold stimulation of PI metabolism over basal levels for each experiment. The data shown are from representative experiments. Curves through the data were derived from a least-squares fit to equation 1. *Top*, wild-type pm2 mAChR (two experiments),  $1.2 \times 10^6$  receptors/cell. Fitted parameters for the control were  $EC_{50} = 2.9 \pm 0.7 \mu M$ , 2-fold. *Middle*, K214A pm2 mAChR mutant (four experiments),  $3.8 \times 10^5$  receptors/cell with fitted parameters of  $EC_{50} = 1.3 \pm 0.7 \mu M$ , 1.7-fold; and  $EC_{50} = 0.08 \pm 0.04$

## Discussion

The i3 loop of G protein-coupled receptors plays an important role in regulating receptor/effector coupling. Deletion mutants of the  $\beta_2$ -adrenergic receptor indicated that the amino- and carboxyl-terminal regions are necessary for coupling to stimulation of adenylyl cyclase (11, 12). Deletion analysis of the third intracellular loop for the m1 mAChR also indicated that the middle 126 amino acids are not necessary for agonist-mediated stimulation of PI metabolism (21). The entire third intracellular loop and part of the fifth transmembrane region were switched in m1/m2 chimeric receptors. When expressed in oocytes, the m1/m2 chimera exhibited the physiological response characteristics of the receptor that contributed the loop (22), also implying a role in specificity.

Other studies indicate that effector specificity is conferred by the first 15–20 amino-terminal amino acids of i3 (8, 9). Wess *et al.* expressed m2/m3 chimeras in A9 L cells where the first 16 (of m2) or 17 (of m3) amino-terminal residues were swapped between the muscarinic receptor subtypes. The m3/m2-16 residue chimera did not couple to PI hydrolysis but did weakly inhibit formation of cAMP via a PTX-sensitive G protein. The m2/m3-17 residue chimera on the other hand coupled to PI metabolism through a PTX-insensitive G protein while maintaining PTX-sensitive inhibition of cAMP formation (8). This implies that the amino-terminal region of i3 plays an important role in determining coupling selectivity but may not be the only determinant. To characterize important residues in this region, single and multiple mutations were introduced in the fifth, seventh, and 12–16th amino-terminal amino acids of i3 in the porcine m2 mAChR. Our findings indicate that subtle changes in G protein-coupling characteristics and ligand-binding parameters can occur with little or no change in observed physiological responses.

A detailed interpretation of the effects of mutations on agonist-binding properties is difficult. We have analyzed agonist competition data assuming models for three classes of noninteracting sites or a two-state model plus a third receptor state that does not couple to G proteins (33). Both approaches allow calculation of values for  $K_1$ , the agonist dissociation constant from the receptor G protein complex, and  $K_2$ , the dissociation constant for agonist binding to the free receptor, as well as  $K_3$ , the agonist dissociation constant from a molecularly undefined receptor state that does not couple to G proteins. The assignment of  $K_1$  and  $K_2$  is based on the conversion of  $F_1$  to  $F_2$  by guanine nucleotides (33). However, both analyses show multiple local minima and appear to be ill conditioned. In addition, models based on equilibrium (37) or kinetic data (38) have been proposed that evoke receptor/receptor interactions. Nevertheless, the data in Table 3 indicate that even single amino acid mutations in a region of the m2 mAChR thought to be involved in coupling to G proteins also affect the ligand-binding properties of the protein.

The effects of the mutations on receptor/effector coupling were more straightforward. Replacing a positively charged residue with a neutral one (K214A) resulted in a receptor

$\mu M$ , 1.5-fold for control and PTX-treated, respectively. *Bottom*, KD-KKE(219–223)ELAAL pm2 mAChR mutant (two experiments),  $1.0 \times 10^6$  receptors/cell with fitted parameters for the control:  $EC_{50} = 15 \pm 10 \mu M$ , 2.5-fold.

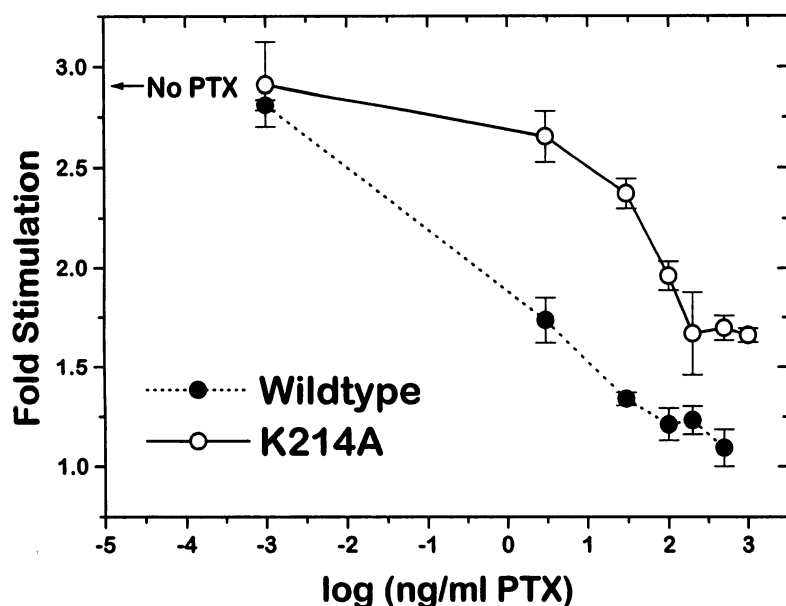


**Fig. 5.** Effect of PTX concentration on maximal IP1 accumulation by wild-type pm2 mAChR and K214A. Cells were treated with various concentrations of PTX for 12 hr before conducting the PI assay and assayed for inositol monophosphate accumulation 50 min after addition of 1 mM carbachol. Data are presented as maximal fold increase in IP1 accumulation over basal levels for PTX-treated as well as control cells. Data shown are the mean of triplicate determinations ( $\pm$  standard deviation) from one representative experiment. The curves through the data have no theoretical basis.

that coupled to effector systems through a different G protein(s). The difference in PTX sensitivity for agonist stimulation of PI metabolism has previously been reported for receptors expressed in CHO cells (5, 23). Three classes of responses were described for both transfected and endogenous receptors. Endogenous receptors for thrombin and transfected porcine m2 mAChRs coupled to PI metabolism by PTX-sensitive G proteins, whereas transfected m1 and m3 receptors were only partially sensitive to PTX, suggesting both PTX-sensitive and -insensitive G proteins mediated the response. On the other hand, endogenous cholecystikinin receptors coupled to PI metabolism through a completely PTX-insensitive G protein (6).

K214A appeared to couple to both inhibition of cAMP formation and stimulation of PI metabolism in a manner similar to wild-type pm2 receptor. Because inhibition of cAMP formation is mediated by a PTX-sensitive G protein for K214A, it is clear that this mutant still efficiently couples to  $G_i$ . It has been demonstrated that wild-type m2 mAChR couples to PI metabolism through the PTX-sensitive G proteins  $G_{\alpha_{i2}}$  and  $G_{\alpha_{i3}}$  in CHO cells (24). This suggests that for K214A, coupling to PI metabolism could occur through  $G_i$  as well as some other PTX-insensitive G protein, perhaps  $G_q$  or  $G_{11}$ .  $G_q$  and  $G_{11}$ , which mediate coupling to PI metabolism in a PTX-insensitive manner, are expressed in our CHO cell line, as are  $G_{\alpha_{i2}}$  and  $G_{\alpha_{i3}}$ , whereas  $G_{\alpha_{i1}}$  and  $G_{\alpha_{\infty}}$  are not expressed (24).<sup>1</sup> After exposure to 100 ng/ml PTX, a concentration sufficient to eliminate coupling to PI stimulation for wild-type, A212E, and KDKKE(219–223)ELAAL, K214A still appeared to couple to this response with an  $EC_{50}$  for carbachol shifted leftward by ~20-fold compared with the non-PTX-treated control. This suggested that the major pathway for IP1 formation was through a different G protein after PTX treatment than in non-PTX-treated controls and that this response appeared to be more tightly coupled in the presence of carbachol. When cells expressing K214A were treated with high concentrations of PTX, the dose-response curve was shifted rightward and complete uncoupling did not occur,

even at high PTX concentrations (Fig. 5). Taken together, these results indicate that K214A must be coupling to PI stimulation through both PTX-sensitive and -insensitive G proteins. Whether the rightward shift of the PTX dose-response curve is due to K214A coupling to a different PTX-sensitive G protein than wild-type receptor or to an increase in coupling through the PTX-insensitive pathway as the levels of PTX-sensitive G protein are reduced is not yet known. When chimeric m1/m2 receptors with i3 or the amino-terminal portion of i3 were reconstituted with specific G proteins ( $G_i$ ,  $G_o$ ,  $G_z$ ,  $G_q$ , and  $G_s$ ), receptor G protein interactions occurred with both PTX-sensitive and -insensitive G proteins (31). An alternative explanation also compatible with this result is that the K214A mutation stabilizes the receptor/G protein complex, reducing the availability of the G protein to PTX.

Lysine is conserved at amino acid position 214 in the m2/m4 mAChR family, whereas the m1/m3/m5 family has a conserved glutamate in that position. Perhaps the positively charged side chain of lysine is important in determining the nature of G protein-coupling interactions for the m2/m4 mAChRs. Replacing this lysine with a neutral alanine may remove a constraint that allows the receptor to interact with multiple G proteins. For the human m3 mAChR, several charged residues near the amino-terminal of i3 were required for normal signal transduction (25).

The amino-terminal region of i3 is predicted to form an amphipathic  $\alpha$ -helical structure in all G protein-coupled receptors. Studies on chimeric m2/m3 mAChRs suggest that receptors with similar function use regions of conserved charge and secondary structure without complete sequence identity (9). Although this motif may represent a structural requirement in receptor/G protein interactions in general, the individual charged residues within this region may play a role in determining the nature of the protein/protein interaction. When the amino acid sequences of the third intracellular loop are aligned, the amino-terminal regions are most conserved among the functional families (e.g., m2/m4 versus m1/m3/m5). Replacing lysine with glutamate at position 214 (K214E), which swaps residues conserved at that position

<sup>1</sup> J. Robishaw, unpublished observations.



between the functional families, resulted in a receptor that was not properly processed. All receptor sites detected ( $3 \times 10^5$  sites/cell) were internalized with no expression on the cell surface (data not shown).

Replacement of a nonpolar amino acid with an acidic one (A212E) resulted in ligand-binding and effector-coupling properties similar to those of wild-type receptor. The notable exceptions were the weaker binding of acetylcholine and that Oxo M appears to be less effective at stimulating PI hydrolysis than other agonists, although it bound with high affinity. Acetylcholine also appeared to be less effective at stimulating PI hydrolysis and is significantly different ( $p \leq 0.01$ ) than wild-type pm2 (Table 1). When normalized to carbachol-stimulated levels of IP1, this reduced efficacy is less striking and does not significantly differ from the full agonist carbachol, whereas Oxo M does (Fig. 1a). It is not clear whether Oxo M promoted a receptor conformation that was in general less efficient at coupling to  $G_i$  or if changes in  $G_{i\alpha}$  subtype selectivity were altered reducing the efficiency of effector activation. Regardless of the mechanism of action, it is significant to note that this finding implies that the agonists Oxo M and, although to a lesser extent, acetylcholine behaved differently than carbachol.

All agonist-mediated physiological responses for A212E in CHO cells occur through PTX-sensitive G proteins, making it difficult to determine whether subtle changes in coupling result. At pm2 mAChR numbers greater than  $10^6$  per cell, maximal stimulation of PI metabolism appeared to be limited by receptor expression, whereas maximal inhibition of cAMP formation was not. Most investigations of receptor mutants are carried out on cell lines that are overexpressing receptor. Under these conditions, inefficient coupling of receptor to  $G_i$  may go unnoticed in assays of cellular cAMP levels since the receptor is in excess. Although Oxo M-mediated inhibition of cAMP formation for A212E resembles wild-type receptor, it is possible that this agonist promotes a receptor conformation that is less efficient at activating the G proteins expressed in CHO cells.

All of the mutant receptors assayed as well as wild-type pm2 mAChR exhibit both inhibition and stimulation of cAMP formation. Although the stimulatory phase is not dependent on  $Ca^{2+}$  or activation of protein kinase C (26), the mechanism by which this effect occurs is not known. For the  $\alpha_2$ -adrenergic receptor, which also couples to both inhibition and stimulation of cAMP formation, the stimulatory phase has been reported to be mediated by a direct interaction with  $G_s$  (27). m4 mAChRs have also been shown to activate  $G_s$  directly in HEK 293 cells (28). These observations implicate an indirect pathway in the stimulation of cAMP formation, possibly mediated by G protein  $\beta\gamma$  subunits.

The KDKKE(219–223)ELAAL pm2 receptor mutant replaced the 12–16th amino-terminal residues conserved in the m2/m4 functional family with those conserved in the m1/m3/m5 family. Although this change introduces alterations in the charge distribution within this domain of i3, it does not affect the predicted secondary structure of this portion of the loop. Binding of carbachol and Oxo M was affected but not effector-coupling characteristics. Coupling to effector systems occurred via PTX-sensitive G proteins as seen in wild-type receptor (Fig. 4). Fold stimulation of PI hydrolysis resembled wild-type pm2 receptor, whereas human m1 mAChRs expressed in CHO cells elicited a 13-fold increase in IP1

accumulation (data not shown). The  $EC_{50}$  values for acetylcholine and carbachol significantly differed from wild-type, whereas the  $EC_{50}$  value for Oxo M did not. Although residues 219–223 are within the region of i3 reportedly responsible for switching effector-coupling characteristics between m2 and m3 mAChRs (8), this finding suggests that charge distribution in this domain of the loop does not play a large role in G protein selectivity. This finding is supported by the converse mutation made in the human m1 mAChR (14) where change in charge distribution played a minor role in G protein coupling to PI metabolism.

The amino-terminal domain of the third intracellular loop of the mAChR appears to play a role in G protein coupling, but it is clearly not the only determinant. Chimeric muscarinic (8–10) and  $\alpha_1$ -adrenergic (29) receptors gain the coupling selectivity of the introduced loop, while characteristics of the wild-type receptor are retained to some degree. The rat m3 mAChR amino-terminal domain of i3 was studied by replacing residues with corresponding amino acids found in the m2/m4 receptor family (34). The authors concluded that a critical tyrosine residue in rat m3 was necessary for efficient coupling to PI hydrolysis, although substitution of tyrosine for serine in the corresponding position of Hm2 did not result in an enhanced PI response (35). Högger *et al.* (32) studied Hm1 amino- and carboxyl-terminal junctions of i3. They proposed that these domains of i3 could function as a crucial hinge region, allowing exposure of specific binding pockets on agonist binding as well as a specific recognition substrate, and they cautioned against the definition of precise coupling domains in these regions of the muscarinic receptor. In addition, the G protein selectivity of chimeric receptors (31) appears to depend on specific contributions by both i2 and i3, and promiscuous receptor G protein interactions occur in the absence of the correct i2.

Because all members of the seven transmembrane receptor family interact with G proteins, it is possible that portions of the transmembrane region (the most well conserved domains) are also important in determining G protein recognition characteristics. A mutation in the second transmembrane region (D69N) results in a pm2 receptor that binds agonists but does not efficiently couple to effectors.<sup>2</sup> The role of intracellular loops may be to modulate coupling to G proteins, and characteristics observed for each receptor system studied may be dependent on the context in which they are expressed. Coupling selectivity and efficiency may be dependent on the interaction of intracellular loops with other structural domains of the receptor as well as those of the specific G proteins expressed in the cells being examined. Mouse m1 AChRs when expressed in Y1 adrenal carcinoma cells, CHO cells, and Rat-2 fibroblasts coupled to multiple G proteins (as determined by differential PTX sensitivity) in a cell line-specific manner (30).

In summary, we have shown that single amino acid changes in the amino-terminal domain of i3 can lead to subtle changes in G protein-coupling characteristics. This finding suggests that analysis of mutants designed to assess coupling selectivity may require more detailed examination before definite conclusions can be drawn. Although it appears that coupling is affected by amino-terminal residues of i3, the nature of these interactions may be determined by several

<sup>2</sup> W. K. Vogel and M. I. Schimerlik, unpublished observation.

structural domains simultaneously rather than by the i3 loop alone as well as the context in which the receptor is expressed. It is imperative that careful evaluation of all data pertaining to coupling characteristics be considered before conclusions be drawn on important structural domains. Elucidation of explicit roles of the structural domains important in G protein coupling by site-directed mutagenesis requires that high resolution assessment of selectivity be used.

#### Acknowledgments

The authors would like to acknowledge the technical assistance of Valerie Mosser and helpful discussions with Walter Vogel, Birgit Hirschberg, David Broderick, and Gary Peterson. We would also like to thank Dr. D. Capon at Genentech for providing the clone of the pm2 mAChR and the pSVE expression vector and Dr. Janet Robishaw for determining the G protein composition of our CHO cell line membranes.

#### References

- Kubo, T., K. Fukuda, A. Mikami, A. Maeda, H. Takahashi, M. Mishina, T. Haga, K. Haga, A. Ichihama, K. Kangawa, M. Kohima, H. Matsuo, T. Hirose, and S. Numa. Cloning, sequencing and expression of complementary DNA encoding the muscarinic acetylcholine receptor. *Nature (Lond.)* **323**:411–416 (1986).
- Bonner, T. I., N. J. Buckley, A. C. Young, and M. R. Brann. Identification of a family of muscarinic acetylcholine receptor genes. *Science (Washington D. C.)* **237**:527–532 (1987).
- Peralta, E. G., J. W. Winslow, D. H. Smith, A. Ashkenazi, J. Ramachandran, M. I. Schimerlik, and D. J. Capon. Primary structure and biochemical properties of an M2 muscarinic receptor. *Science (Washington D. C.)* **236**:600–605 (1987).
- Hulme, E. C., N. J. M. Birdsall, and N. J. Buckley. Muscarinic receptor subtypes. *Annu. Rev. Pharmacol. Toxicol.* **30**:633–673 (1990).
- Ashkenazi, A., J. W. Winslow, E. G. Peralta, G. L. Peterson, M. I. Schimerlik, D. J. Capon, and J. Ramachandran. An M2 muscarinic receptor subtype coupled to both adenylyl cyclase and phosphoinositide turnover. *Science (Washington D. C.)* **238**:672–675 (1987).
- Ashkenazi, A., E. G. Peralta, J. W. Winslow, J. Ramachandran, and D. J. Capon. Functional diversity of muscarinic receptor subtypes in cellular signal transduction and growth. *Trends Pharmacol. Sci. Dec. Suppl.*: 16–22 (1989).
- Wess, J., M. R. Brann, and T. I. Bonner. Identification of a small intracellular region of the muscarinic m3 receptor as a determinant of selective coupling to PI turnover. *FEBS Lett.* **258**:133–136 (1989).
- Wess, J., T. I. Bonner, F. Dorje, and M. R. Brann. Delineation of muscarinic receptor domains conferring selectivity of coupling to guanine nucleotide-binding proteins and second messengers. *Mol. Pharmacol.* **38**:517–523 (1990).
- Lechleiter, J., R. Helmiss, K. Duerson, D. Ennulat, N. David, D. Clapham, and E. G. Peralta. Distinct sequence elements control the specificity of G protein activation by muscarinic acetylcholine receptor subtypes. *EMBO J.* **9**:4381–4390 (1990).
- Bonner, T. I. Domains of muscarinic acetylcholine receptors that confer specificity of G protein coupling. *Trends Pharmacol. Sci.* **13**:48–50 (1992).
- Dixon, R. A., I. S. Sigal, E. Rands, R. B. Register, M. R. Candelore, A. D. Blake, and C. D. Strader. Ligand binding to the  $\beta$ -adrenergic receptor involves its rhodopsin-like core. *Nature (Lond.)* **326**:73–77 (1987).
- Strader, C. D., R. A. F. Dixon, A. H. Cheung, M. R. Candelore, A. D. Blake, and I. S. Sigal. Mutants that uncouple the  $\beta$ -adrenergic receptor from Gs and increase agonist affinity. *J. Biol. Chem.* **262**:16439–16443 (1987).
- Bonner, T. I. New subtypes of muscarinic acetylcholine receptors. *Trends Pharmacol. Sci.* **10**:11–15 (1989).
- Arden, J. R., O. Nagata, M. S. Shockley, M. Philip, J. Lamah, and W. Sadee. Mutational analysis of third cytoplasmic loop domains in G protein coupling of the HM1 muscarinic receptor. *Biochem. Biophys. Res. Commun.* **188**:1111–1115 (1992).
- Sanger, F., Nicklen, S., and A. R. Coulson. DNA sequencing with chain terminating inhibitors. *Proc. Natl. Acad. Sci. USA* **74**:5463–5467 (1977).
- Peterson, G. L., and M. I. Schimerlik. Large scale preparation and characterization of membrane-bound and detergent solubilized muscarinic receptor from pig atria. *Prep. Biochem.* **14**:33–74 (1984).
- Lee, W., K. J. Nicklaus, D. R. Manning, and B. B. Wolfe. Ontogeny of cortical muscarinic receptor subtypes and muscarinic receptor-mediated responses from rat. *J. Pharmacol. Exp. Ther.* **252**:482–490 (1990).
- Salomon, Y. Adenylate cyclase assay. *Adv. Cyclic Nucleotide Res.* **10**:35–55 (1979).
- Tota, M. R., K. R. Kahler, and M. I. Schimerlik. Reconstitution of the purified porcine atrial muscarinic acetylcholine receptor with purified porcine atrial inhibitory guanine nucleotide binding protein. *Biochemistry* **26**:8175–8182 (1987).
- Scatchard, G. The attractions of proteins for small molecules and ions. *Ann. N. Y. Acad. Sci.* **51**:660–672 (1949).
- Shapiro, R. A., and N. M. Nathanson. Deletion analysis of the mouse m1 muscarinic acetylcholine receptor: effects on phosphoinositide metabolism and down-regulation. *Biochemistry* **28**:8946–8950 (1989).
- Kubo, T., H. Bujo, I. Akiba, J. Nakai, M. Mishina, and S. Numa. Location of a region of the muscarinic acetylcholine receptor involved in selective effector coupling. *FEBS Lett.* **241**:119–125 (1988).
- Ashkenazi, A., E. G. Peralta, J. W. Winslow, J. Ramachandran, and D. J. Capon. Functionally distinct G proteins selectively couple different receptors to PI hydrolysis in the same cell. *Cell* **56**:487–493 (1989).
- Dell'Acqua, M. L., R. C. Carroll, and E. G. Peralta. Transfected m2 muscarinic acetylcholine receptors couple to Gai2 and Gai3 in Chinese hamster ovary cells: activation and desensitization of the phospholipase C signaling pathway. *J. Biol. Chem.* **268**:5676–5685 (1993).
- Kunkel, M. T., and E. G. Peralta. Charged amino acids required for signal transduction by the m3 muscarinic acetylcholine receptor. *EMBO J.* **12**: 3809–3815 (1993).
- Baumgold, J. Muscarinic receptor-mediated stimulation of adenylyl cyclase. *Trends Pharmacol. Sci.* **13**:339–340 (1992).
- Eason, M. G., H. Kurose, B. D. Holt, J. R. Raymond, and S. B. Liggett. Simultaneous coupling of  $\alpha$ 2-adrenergic receptors to two G proteins with opposing effects. *J. Biol. Chem.* **267**:15795–15801 (1992).
- Dittman, A. H., J. P. Weber, T. R. Hinds, E.-J. Choi, J. C. Migeon, N. M. Nathanson, and D. R. Storm. A novel mechanism for coupling of m4 muscarinic acetylcholine receptors to calmodulin-sensitive adenylyl cyclases: crossover from G protein-coupled inhibition to stimulation. *Biochemistry* **33**:943–951 (1994).
- Cotecchia, S., J. Ostrowski, M. A. Kjelsberg, M. G. Caron, and R. J. Lefkowitz. Discrete amino acid sequences of the  $\alpha$ 1-adrenergic receptor determine the selectivity of coupling to phosphatidylinositol hydrolysis. *J. Biol. Chem.* **267**:1633–1639 (1992).
- Shapiro, R. A., D. Palmer, and T. Cislo. A deletion mutation in the third cytoplasmic loop of the mouse m1 muscarinic acetylcholine receptor unmasks cryptic G protein binding sites. *J. Biol. Chem.* **268**:21734–21738 (1993).
- Wong, S., and E. M. Ross. Chimeric muscarinic cholinergic:  $\beta$ -adrenergic receptors that are functionally promiscuous among G proteins. *J. Biol. Chem.* **269**:18968–18976 (1994).
- Högger, P., M. S. Shockley, J. Lamah, and W. Sadee. Activating and inactivating mutations in N- and C-terminal i3 loop junctions of muscarinic acetylcholine Hm1 receptors. *J. Biol. Chem.* **270**:7405–7410 (1995).
- Vogel, W. K., V. A. Mosser, D. A. Bulseco, and M. I. Schimerlik. Porcine m2 muscarinic acetylcholine receptor-effector coupling in Chinese hamster ovary cells. *J. Biol. Chem.* **270**:15485–15493 (1995).
- Blüml, K., E. Mutschler, and J. Wess. Identification of an intracellular tyrosine residue critical for muscarinic receptor-mediated stimulation of phosphatidylinositol hydrolysis. *J. Biol. Chem.* **269**:402–405 (1994).
- Blüml, K., E. Mutschler, and J. Wess. Functional role of a cytoplasmic aromatic amino acid in muscarinic receptor-mediated activation of phospholipase C. *J. Biol. Chem.* **269**:11537–11541 (1994).
- Barlow, R., and J. F. Blake. Hill coefficients and the logistic equation. *Trends Pharmacol. Sci.* **10**:440–441 (1989).
- Chidiac, P., and J. W. Wells. Effects of adenylyl nucleotides and carbachol on cooperative interactions among G proteins. *Biochemistry* **31**:10908–10921 (1992).
- Hirschberg, B. T., and M. I. Schimerlik. A kinetic model for oxotremorine M binding to recombinant porcine m2 muscarinic receptors expressed in Chinese hamster ovary cells. *J. Biol. Chem.* **269**:26127–26135 (1994).
- Bevington, P. R. *Data Reduction and Error Analysis for the Physical Sciences*. McGraw-Hill Book Co., New York, 56–65 (1969).

Send reprint requests to: Dr. Michael I. Schimerlik, Department of Biochemistry and Biophysics, Oregon State University, Corvallis, OR 97331.